Electrochemically-assisted deposition of oxidases on platinum nanoparticle/multi-walled carbon nanotube-modified electrodes

Male, Keith B.; Hrapovic, Sabahudin; Luong, John H. T.

Publisher's version / Version de l'éditeur:

The Analyst, 132, 12, pp. 1254-1261, 2007

Electrochemically-assisted deposition of oxidases on platinum nanoparticle/multi-walled carbon nanotube-modified electrodes

Keith B. Male, Sabahudin Hrapovic and John H. T. Luong*

Received 14th August 2007, Accepted 19th September 2007
First published as an Advance Article on the web 28th September 2007
DOI: 10.1039/b712478c

Platinum nanoparticles were electrodeposited by a multi-potential step technique onto a multi-walled carbon nanotube (MWCNT) film pre-casted on a glassy carbon (GC) or boron-doped diamond (BDD) electrode. The MWCNT network consisted of Pt nanoparticles with an average diameter of 120 nm after an optimization of 36 deposition cycles. The resulting electrochemical sensors were capable of detecting hydrogen peroxide as low as 25 nM. Five different enzymes: glucose, lactate, glutamate, amino acid and xanthine oxidases, respectively, were deposited by a constant current technique for 5–10 min to form a stable and active biolayer for the analysis of their corresponding analytes. The glucose oxidase-based biosensor was linear up to 10 mM glucose with a detection limit of 250 nM and a response time of 5 s. Similar response times and detection limits were observed with glutamate, lactate, and amino acid oxidase despite the fact that the linear ranges were noticeably narrower. The mechanism of deposition was attributed to the decrease of local pH, created by oxygen evolution and effected enzyme precipitation.

Introduction

Immobilization of a sensing biomolecule on the transducer surface with high activity and reproducibility is one of the important steps in biosensor construction. Among various procedures, electrochemical deposition is appealing since it can be applied to any electrode surface morphology in one or two rapid steps. In a microfabricated array format, this procedure allows for the deposition of different proteins in various electro-addressable parts of the array. The most popular strategy is the co-deposition of the biomolecule with an electropolymerizable monomer such as pyrrole, phenol and its derivatives, 1,3-diaminobenzene, *etc.*, to form an insoluble matrix for enzyme entrapment.[1] Within this procedure, the biomolecule can be pre-conjugated with such a monomer to promote electropolymerization.[2] To overcome mass transfer diffusion, especially for high molecular weight analytes such as antibodies, proteins, *etc.*, the biomolecule can be covalently attached to the electropolymerized film formed on the active area of an electrode.[3] Another possibility is the co-deposition of the biomolecules with a platinum salt[4] or with another protein such as bovine serum albumin, collagen,[5] *etc.* Regardless of the procedure used, the ultimate goal is to immobilize the biomolecule in its native active state to form a stable and reusable biolayer with high reproducibility.

The quest for electrochemical detection of important analytes with very low detection limits with high specificity has intensified with several avenues being explored. Carbon nanotubes (CNTs) have become an extremely popular theme in recent electrochemical sensing research because of their nanoscale diameter, high electrocatalytic activity, and decreased vulnerability to surface fouling. CNTs can be used as electrode materials with useful properties for various potential applications including miniature biological devices. The subject of electrochemical sensing using carbon nanotubes has been extensively studied and reviewed by various authors.[6] In general, CNTs promote electron-transfer reactions at low overpotentials and this distinct feature has inspired increased research in coupling CNT-based sensors with enzymes. A significant amount of work in the area of enzyme biosensors is related to CNTs because H_2O_2 is released during the oxidation of the substrate by a pertinent oxidoreductase. For example, many glucose-based biosensors have been designed by integrating glucose oxidase (GOx) with CNTs.[6d–g] Incorporating glucose oxidase with single-walled CNTs (SWCNTs) derivatized with suitable redox mediators such as ferrocene or poly[(vinylpyridine)$Os(bipyridyl)_2Cl^{2+/3+}$] has been used recently to construct glucose biosensors.[6h,i] Hydrogen peroxide is also an important intermediate species in many biological processes. Oxidative damages resulting from the cellular imbalance of H_2O_2 and other reactive oxygen species are connected to aging and severe human diseases including cancers and cardiovascular disorders.[6j] Cancer cells that are resistant to cisplatin or other cancer therapies, such as radiation, seem to synthesize larger amounts of peroxiredoxin which degrades hydrogen peroxide.[6k] Therefore, the detection of H_2O_2 is of interest to many fields in analytical and biomedical chemistry.

This study describes the possibility of the electrochemically-assisted deposition of five important oxidases including glucose oxidase, on GC or BDD electrodes which have been modified with CNTs and then Pt nanoparticles. The use of Pt nanoparticles together with CNTs has been known to enhance the detection of H_2O_2, a by-product of the enzymatic oxidation.[7] Since their discovery,[8] CNT-based chemical/biochemical sensors are promising for detecting molecules in the gas or liquid phase since biomolecules can be trapped

Biotechnology Research Institute, National Research Council Canada, Montreal, Quebec, Canada H4P 2R2

inside and placed onto the outer surfaces of open-ended CNTs.[9] For instance, streptavidin is adsorbed on CNTs presumably *via* hydrophobic interactions between CNTs and hydrophobic domains of the proteins,[10] whereas DNA is adsorbed on CNTs *via* non-specific interactions.[8] Notice that GOx can be electrochemically deposited on a bare Pt electrode; however, a detergent (Triton® X-100) above its critical micelle concentration (CMC) must be present to produce a multi-layered deposit.[11] Although the procedure is applicable for robust GOx with high activity, the presence of such a detergent above its CMC level might denature or at least adversely affect the activity of other fragile biomolecules. To our knowledge, this is the first attempt to electrochemically deposit enzyme on electrodes which have been modified with CNTs and Pt nanoparticles towards the development of biosensing platforms for oxidases. It has been seen that electropolymerized films exhibit significantly different characteristics when formed on different electrode materials and under different electropolymerization conditions.[12]

Experimental

Materials

Dihydrogen hexachloroplatinate(IV) hexahydrate ($H_2PtCl_6 \cdot 6H_2O$) was purchased from Alfa Aesar (Ward Hill, MA). Multi-walled carbon nanotubes (MWCNTs, 95%, 10–20 nm diameter, 1–5 μm length) were obtained from NanoLab (Brighton, MA), while single-walled CNTs (SWCNTs) were obtained from Carbon Nanotechnology (Houston, TX). Glucose oxidase (GOx, type X-S: *Aspergillus niger*, 185 U mg^{-1}, a dimer consisting of two equal subunits with a molecular weight of 80 kDa each, where each subunit contains one mole of flavin adenine dinucleotide (FAD) and one mole of iron), lactate oxidase (LOx, *Pediococcus* species, 34 U mg^{-1}, a flavin mononucleotide (FMN)-containing enzyme and a member of the α-hydroxy-acid oxidase flavoenzyme family with a molecular weight of 80 kDa), L-amino acid oxidase (AAOx, *Crotalus atrox*, 0.7 U mg^{-1}, consisting of two different subunits of approximately 70 kDa with two FAD molecules per molecule of holoenzyme), xanthine oxidase (XOx, bovine milk, 1.3 U mg^{-1}, a homodimer consisting of two equal subunits of 140 kDa, where each subunit contains one mole of FAD, one atom of Mo, and four iron atoms), glucose, glutamate, phenylalanine, lactate, hypoxanthine, hydrogen peroxide, Triton® X-100, Nafion®-perfluorinated ion-exchange resin (5% wt), and all other chemicals were purchased from Sigma-Aldrich (St. Louis, MO) and used without any further purification. Glutamate oxidase (GLOx, *Streptomyces* sp. X119-6, 25 U mg^{-1}, 140 kDa) was obtained from Yamasa Corp. (Coshi, Japan). This enzyme consists of two α-chains, two β-chains, and two γ-chains of respective subunit molecular weights of about 44, 19 and 9 kDa. It contains 2 mol of flavin adenine dinucleotide (FAD) per mole of enzyme. All solutions were prepared using Milli-Q (Millipore, Bedford, MA) A-10 gradient (18 MΩ·cm) deionized water.

Instrumentation

Cyclic voltammetry (CV) and amperometric (*I*/*t*) measurements were performed using an electrochemical analyzer (CHI 601A, CHI Instruments, Austin, TX). Pt nanoparticle and enzyme electrodeposition was carried out using an electrochemical workstation (CHI 760B, CHI Instruments, Austin, TX). Pt nanoparticle coverage over the MWCNT layer was analyzed using CV mode at a scan rate of 100 mV s^{-1} with a potential window between −0.60 and +1.20 V. These conditions allow for the observation of hydrogen adsorption/desorption and oxygen formation/reduction peaks, both characteristic of Pt surfaces in 50 mM phosphate buffer at pH 6. The stability of the formed Pt nanoparticle/MWCNT layer on GC surfaces was verified by multiple cycling (minimum 40 runs) under the above-mentioned conditions. Analyte detection was performed in amperometric (*I*/*t*) mode applying a fixed potential of 0.70 V in 50 mM phosphate buffer pH 6 for glucose, pH 6.5 for glutamate, lactate, and phenylalanine and pH 7.5 for hypoxanthine, the pH optima for the corresponding enzymes. All electrochemical measurements were performed in a 30 mL EG&G PARC electrochemical cell at room temperature. Enzyme-modified electrodes were stored at 4 °C for long-term stability experiments. The electrolyte (10 mL) was magnetically stirred at 450 rpm during the analyte detection to ensure the efficient mixing with the electrolyte. The various analytes were then added once a stable background current was attained. A Pt wire (Aldrich, 99.9% purity, 1 mm diameter) and an Ag/AgCl (3M NaCl) electrode (BAS, West Lafayette, IN) were used as counter and reference electrodes, respectively. Glassy carbon, GC, (3 mm in diameter, BAS) and boron-doped diamond (BDD, 3 mm in diameter, 0.1% doped boron, Windsor Scientific, Slough, Berkshire, UK) modified electrodes served as the working electrode. SEM images were obtained using a Hitachi scanning electron microscope (S-2600 N, Tokyo, Japan) operating in high vacuum mode at acceleration voltages of 5–16 kV and working distances of 3–5 mm. The entire GC electrode was inserted into the SEM chamber and grounded with copper adhesive tape (3M, St. Paul, MN) to reduce ionization. Nanoparticle size was determined from SEM images, magnifications between 25 000 and 30 000× using Scion Image (Scion, Frederick, MD).

Electrode preparation and CNT film formation

GC and BDD working electrodes were first cleaned with wet silicon carbide paper, grit 1500 (Hand American Made Hardwood Products, South Plainfield, NJ), followed by polishing with 0.05 μm alumina slurry (Buehler, Markham, ON, Canada) on velvet using a model 900 grinder/polisher (South Bay Technol., San Clemente, CA). After rinsing thoroughly with deionized water, the electrodes were sonicated for 5 min to remove excess alumina followed by a 5 min treatment in Piranha solution (70% sulfuric acid, and 30% hydrogen peroxide). After sonication for another 5 min in deionized water, the conditioned working electrodes were dried under nitrogen and used for modification.

MWCNTs were suspended in *N*,*N*-dimethylformamide (A&C American Chemicals, Montreal, QC, Canada). For electrode preparation, 2 mg mL^{-1} of MWCNTs was used; however, for optimization studies experiments were also performed at 0.25, 0.50, 1.0 and 1.5 mg mL^{-1}. About 2 h of sonication was necessary to obtain well-dispersed MWCNTs.

The MWCNT slurry (20 μL) was applied to the GC or BDD electrode surface and dried for 2 h. For comparison, a slurry of SWCNTs (1 mg mL^{-1}) was also prepared.

Pt nanoparticle electrodeposition on the CNT film

Pt nanoparticles were deposited from a 2 mM H_2PtCl_6 solution in 0.5 M H_2SO_4 onto the CNT-modified GC or BDD electrodes by a multi-potential step electrodeposition technique,[13] using an electrochemical workstation (CHI 760B, CHI Instruments, Austin, TX). In brief, this procedure applied a reduction potential (−0.3 V) for a fixed period (1 s), followed by a relaxation potential (1.3 V for 5 s) in repeated cycles, resulting in stable Pt nanoparticles, with controllable size and density. The number of cycles was optimized by comparing the signal response to glucose after the electrodeposition of a fixed amount of GOx.

Deposition of enzyme and analyte detection

GOx was deposited (CHI 760B, CHI Instruments, Austin, TX) galvanostatically[1j] by applying a constant current of 10 μA on GC and BDD electrodes modified by MWCNTs and Pt nanoparticles. The deposition time (0.25–15 min) and the enzyme concentration (0.16–16 mg mL^{-1}, 30–3000 U mL^{-1}) were optimized. Under optimal conditions, a calibration curve was established for glucose (250 nM to 10 mM) to determine the detection limit and response time. Reproducibility and long-term stability of the electrode were determined at 5 and 500 μM glucose. For comparison, electrode surfaces without Pt nanoparticles (MWCNTs only), as well as surfaces without CNTs (Pt nanoparticles only) were performed with GOx. Similarly, deposition of the other oxidases was optimized.

Results and discussion

Electrochemical deposition of Pt nanoparticles

The distribution, size and number of Pt nanoparticles deposited on the MWCNT (2 mg mL^{-1}) modified electrode surfaces during nucleation followed by particle growth was governed by the Pt salt concentration and the number of deposition cycles. The two-step potential program was performed on electrodes at different numbers of cycles until an optimal signal towards glucose oxidation was obtained. In each case, GOx (8 mg mL^{-1}, 1480 U mL^{-1}) was deposited after the Pt deposition step was completed. Fig. 1 shows that the maximum signal for 10 mM glucose was observed at about 36 cycles. SEM imaging indicated that increasing the number of deposition cycles from 18 to 36 increased the nanoparticle size as well as the nanoparticle distribution (Fig. 2). Pt nanoparticles ranged from 50 to 185 nm at 36 cycles with an average size of 118 ± 10 nm [95% confidence interval (CI), n = 56]. As expected with a lower number of deposition cycles (18) the Pt nanoparticles were smaller, ranging from 40 to 150 nm with an average value of 76 ± 9 nm (95% CI, n = 38). The appearance of Pt electrochemical characteristics was clearly observed with an increase in the number of deposition cycles (Fig. 3). The optimal concentration of Pt salt for 36 deposition cycles was 2–4 mM (figure not shown). The Pt oxide reduction peak at −0.1 V began to decrease as the Pt salt concentration was reduced. At 0.5 mM, the response signal for 10 mM

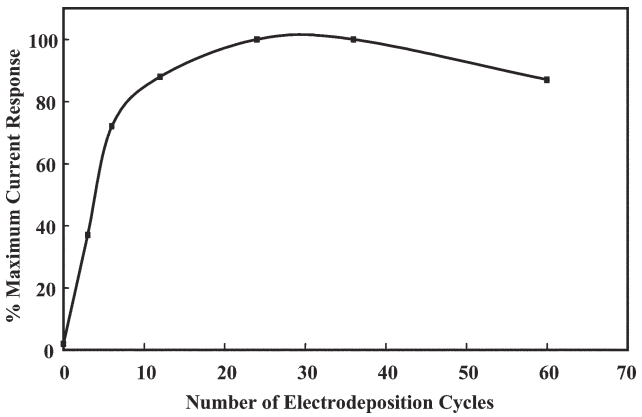

Fig. 1 Effect of the number of platinum electrodeposition cycles (deposition potential E_d = −0.3 V for 1 s, followed by 5 s at the relaxation potential of E_r = 1.3 V) on the glucose (10 mM) signal of a MWCNT-modified GC electrode. Glucose oxidase (GOx, 1480 U mL^{-1}) was deposited on the modified electrode surface after platinum electrodeposition.

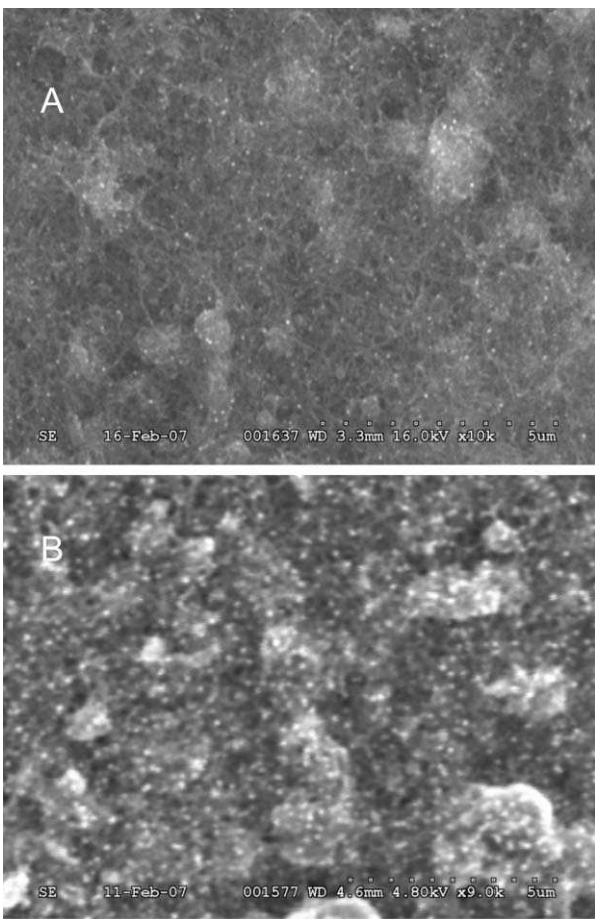

Fig. 2 SEM image of MWCNT-modified GC electrode taken after electrochemical deposition of Pt nanoparticles: (**A**) 18 cycles, acceleration voltage of 16 kV at a working distance of 3.3 mm with magnification of 10 000×; (**B**) 36 cycles, acceleration voltage of 4.8 kV at a working distance of 4.6 mm with magnification 9000×.

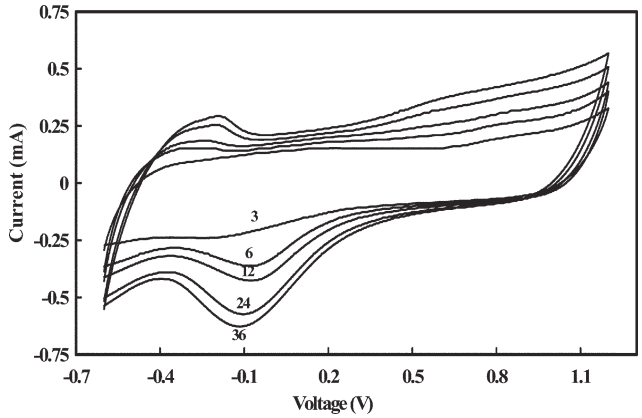

Fig. 3 Cyclic voltammetry (CV) of MWCNT-modified electrode surface after electrodeposition of Pt nanoparticles in 0.1 M phosphate buffer pH 7.0, at a scan rate of 100 mV s^{-1}. The number of cycles is indicated on the figure.

glucose was only 70% of the maximum response. Hence, 2 mM Pt salt was used for all subsequent experiments. Without MWCNTs, the GC surface was well covered by Pt nanoparticles (average size = 138 $\pm$ 19 nm, 95% CI with n = 36, magnification of 18 000 $\times$) after only 6 cycles. A similar result was reported for the deposition of Pt nanoparticles on BDD electrodes.[13b] Apparently, the electrochemical deposition of Pt nanoparticles on the modified MWCNT/GC surface was a much slower process compared with the bare GC electrode. However, the deposition of Pt nanoparticles on bare GC electrodes was not very reproducible. In addition, the signal for 10 mM glucose was 1000-fold smaller (300 nA *vs.* 300 μA) and the detection limit was 80-fold higher (20 μM *vs.* 250 nM) in comparison to the MWCNT-modified GC electrode. These results clearly indicated that GOx adhered firmly to the MWCNT/Pt_{nano}-modified GC surface.

Without GOx, only a very weak signal (2 μA) for 10 mM glucose was observed for the MWCNT/Pt_{nano}-modified GC electrode compared to 300 μA for a MWCNT/Pt_{nano}/GOx-modified electrode. In the absence of Pt_{nano}, a weak signal (6 μA) was also noted for 10 mM glucose and the sensitivity of this MWCNT/GOx-modified electrode was somewhat better than that reported by Liu *et al.*[14] using GOx adsorbed on CNT-modified GC electrodes using ionic liquid. Without the enzyme or Pt nanoparticles, the response to glucose was not observed for the GC or CNT-modified GC electrode. It should be noted that direct glucose oxidation on platinum surfaces is feasible and hydrogen peroxide can be directly detected by MWCNTs. In this study, about 1.5 μA was observed for 100 μM H_2O_2 by the MWCNT-modified GC electrode compared to 30 μA for the MWCNT/Pt-modified GC electrode. A linear relationship between current response and H_2O_2 was observed up to 2.5 mM, with a sensitivity of 272 $\pm$ 1.5 μA mM^{-1} (n = 9, 95% CI), correlation coefficient (R^2) of 0.999 and a detection limit of 25 nM.

Optimization of glucose detection using the MWCNT/Pt_{nano}/GOx-modified GC electrode

FAD is the prosthetic group of many oxidases, including glucose oxidase and all the oxidases used in this study. Such enzymes require molecular oxygen as the co-substrate, which reoxidizes the $FADH_2$ to form H_2O_2 [reactions (1) and (2)] that can be detected amperometrically [reaction (3)]. Substrate diffusion is not limiting since the enzyme is electrochemically deposited on the sensing area of the electrode.

$$\text{Substrate} + H_2O + \text{Enzyme/FAD} \rightarrow \text{Product} + \text{Enzyme/}FADH_2 \quad (1)$$

$$\text{Enzyme/}FADH_2 + O_2 \rightarrow \text{Enzyme/FAD} + H_2O_2 \quad (2)$$

At the electrode

$$H_2O_2 \rightarrow O_2 + 2H^+ + 2e^- \quad (3)$$

When the concentration of the co-substrate oxygen is constant, the current density for the biosensor response, J_{sub}, is a measure of the overall rate of the enzyme reaction, and J_{max} is the J_{sub} value at enzyme saturation. Different values of J_{max}, determined under the same conditions, reflect differences in the amount of active enzyme on the surface, provided that the sensitivity of the electrode to H_2O_2 [reaction (3)] does not vary.

$$J_{sub} = J_{max}/(1 + K_M/[S]) \quad (4)$$

The Michaelis constant, K_M, is defined in terms of the rate constants for the generalized reactions, describing the conversion of substrate (S) to product (P), catalyzed by enzyme (E). Eqn (4) thus illustrates that the reaction kinetics are governed by the amount of active enzyme, the type of enzyme (K_M) and the substrate concentration ([S]).

A series of experiments was conducted to examine the effect of the GOx concentration ($\propto J_{max}$) used for the electrochemical deposition (Fig. 4). Since the response signal obtained for 10 mM glucose (S) became maximal at 8 mg mL^{-1} or 1480 U mL^{-1} GOx, this enzyme level was used for all subsequent studies. The high concentration of enzyme required for signal saturation of glucose was not surprising since the Michaelis constant (K_M) for GOx from *A. niger* is very high (33 mM). The MWCNT concentration used to modify the GC electrode also affected the glucose

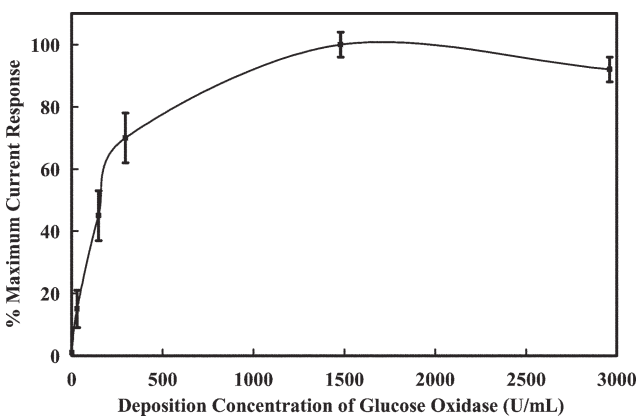

Fig. 4 Effect of the glucose oxidase concentration on glucose (10 mM) detection for the MWCNT/Pt_{nano}-modified GC electrode. 2 mg mL^{-1} MWCNTs and 36 cycles of platinum nanoparticle electrochemical deposition were applied.

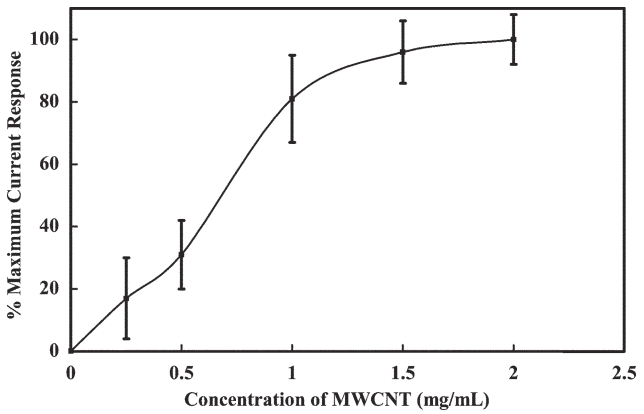

Fig. 5 Effect of the MWCNT concentration on glucose (10 mM) detection for the Pt_{nano}/GOx-modified GC electrode. 1480 U mL^{-1} glucose oxidase (GOx) and 36 cycles of platinum nanoparticle electrochemical deposition were applied.

signal as illustrated in Fig. 5. With optimal results obtained at 2 mg mL^{-1}, this CNT concentration was used for MWCNT film deposition with the response signal obtained within 5 s. The MWCNTs act as nanoconnectors between the Pt nanoparticles and the electrode, resulting in an increase in the electroactive surface area as the concentration of CNTs increases and similar results have been previously reported.[7] Attempts to construct a Pt_{nano}-modified GC electrode with 1 mg mL^{-1} SWCNTs were not successful since the response signal for 10 mM glucose was only 4 μA, *i.e.* 100-fold lower than with MWCNTs. The rationale behind such behavior was not understood but MWCNTs are conductive whereas SWCNTs behave like a semi-conductor. The electrochemically-assisted deposition time for GOx also affected the current signal for 10 mM glucose as shown in Fig. 6. The maximum signal was observed after just 2 min and a time of 5 min was selected for all subsequent experiments. Instead of electrodeposition, a response signal of 40% of the maximum was observed by simply soaking (0 min deposition) the modified electrode in GOx solution for 5 min. Such a result was not

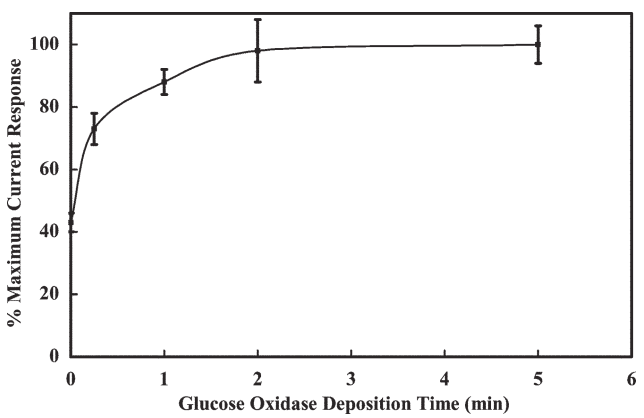

Fig. 6 Effect of the deposition time for glucose oxidase (GOx) on glucose (10 mM) detection for the MWCNT/Pt_{nano}/GOx-modified GC electrode. 2 mg mL^{-1} MWCNTs, 1480 U mL^{-1} GOx and 36 cycles of platinum nanoparticle electrochemical deposition were applied. Deposition current was 10 μA.

completely unexpected since the enzyme could interact with CNTs *via* its hydrophobic domains. However, electrodeposition could produce more extensive and compact enzyme deposit with high reproducibility as suggested by Matsumoto *et al.*[11] As pointed out by Im *et al.*,[15] and later concurred by Matsumoto *et al.*,[11] the driving force for enzyme immobilization was the precipitation of the enzyme on the electrode owing to a decrease in local pH, a result of the oxidation of water. Compared to that of the supporting electrolyte, the electrophoretic mobility of the enzyme during the course of electrodeposition could be neglected.[11]

A wide range, 10–100 μA was observed (figure not shown) for the optimum current of the electrochemical deposition of GOx, thus 10 μA was used for all subsequent studies. At lower currents (2 μA), the signal for 10 mM glucose was only 30% of that at the higher currents. The galvanostatic deposition method (constant current) has been reported to provide higher electrochemical activity for films in comparison to cyclovoltammetric (CV) and potentiostatic deposition methods.[1j] The voltage developed increased from 0.7 to 1.4 V as the current was increased from 2 to 100 μA. Enzyme electrodeposition using the potentiostatic technique at voltages over 1.2 V has been reported;[11] however, significant loss of sensitivity to hydrogen peroxide occurs due to platinum oxide formation. Such behavior was not observed with the constant current technique in the presence of MWCNTs. The detergent Triton® X-100 has been utilized to overcome some of these problems encountered with potentiostatic electrodeposition.[11] In this study, when Triton® X-100 (0.5–2.0 mM) was added to the GOx solution with constant current electrodeposition of GOx onto MWCNT/Pt_{nano}-modified electrodes, the response signal for 10 mM glucose decreased about 50%, which could be attributed to the formation of an increased film thickness. In view of its inferior performance, no attempt was made to characterize such a thick film. However, Matsumoto *et al.*[11] reported that the deposited enzyme layer in the presence of this detergent is about 25 times thicker than the result obtained for the deposition involving only the enzyme (480 nm *vs.* 25 nm). The optimal applied potential to the modified working electrode ranged from 0.5 to 0.7 V (figure not shown). At lower potentials the signal for glucose dropped, whereby at 0.3 V the signal decreased about 50% and at 0.25 V the response signal was negligible.

Glucose calibration

A linear relationship between current response and glucose concentration was observed up to 10 mM (Fig. 7A), with a sensitivity of 30.2 $\pm$ 0.5 μA mM^{-1} (n = 15, 95% CI, R^2 = 0.999) and a detection limit of 250 nM (Fig. 7A inset). The response signal for 20 mM glucose was 1.5-fold higher than at 10 mM. The detection limit was 10-fold higher and the sensitivity was 10-fold lower than the values reported previously for H_2O_2, but still indicated a significant conversion rate. The detection limit and linear range compare favorably to recently reported CNT-based glucose biosensors. For example, a flow injection glucose biosensor based on self-assembling glucose oxidase on MWCNTs reported a detection limit of 15 μM and linearity to 6 mM.[16] In the case of self-assembling

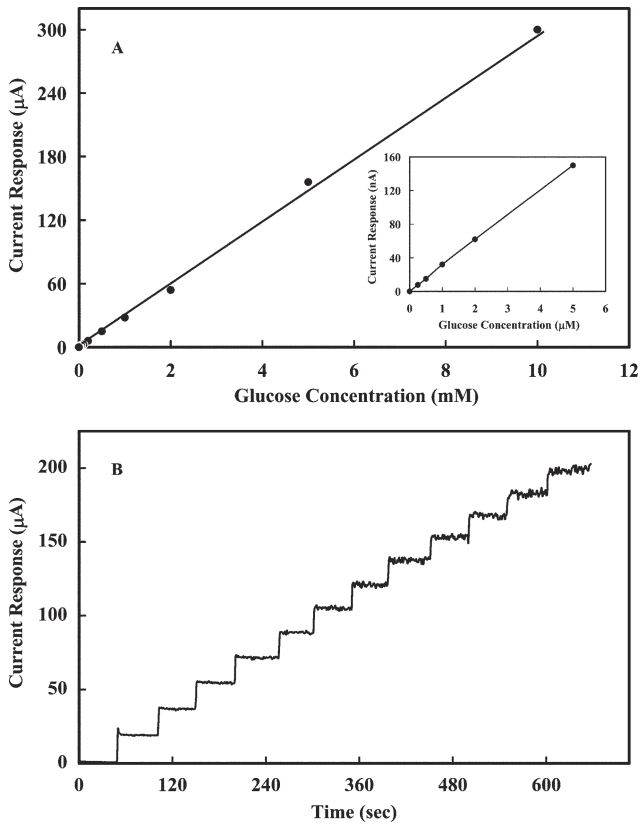

Fig. 7 (**A**) Calibration plot for glucose using the MWCNT/Pt_{nano}/GOx-modified GC electrode. The inset shows the calibration plot at low glucose concentration. (**B**) Repeated analyses of 500 μM glucose using optimal conditions.

glucose oxidase and dendrimer-encapsulated Pt nanoparticles on MWCNTs a detection limit of 2.5 μM and a linear range of 5 μM–0.65 mM was reported.[17] Linearity to 10 mM and a detection limit of 10 μM was achieved with glucose oxidase immobilized in an electropolymerized poly(*o*-aminophenol) CNT film on a gold electrode.[18] Covalent attachment of glucose oxidase to MWCNTs resulted in a detection limit of 30 μM and linearity up to 40 mM.[19] Excellent reproducibility (2–6% at 95% CI) was obtained for the detection of 12 repeated glucose analyses with the modified electrode at 500 μM (16.3 ± 0.9 μA) as observed in Fig. 7B and at 5 μM (0.152 ± 0.003 μA). For a freshly prepared enzyme electrode, a stable baseline was attained within 2 min for the measurement of very low glucose (500 nM) concentrations. Reproducibility (3%) from electrode-to-electrode preparation was considered very satisfactory (294 ± 10 μA for 10 mM glucose, n = 11). The modified electrodes were stable for at least two months and since GOx is a very stable enzyme, longer-term stability was not conducted. For the analysis of glucose from 'real world' samples, for instance, blood or food samples, upon the enzyme deposition, it was necessary to apply a thin layer of Nafion® (5% wt, 10μL, dried on air) in order to circumvent electroactive interferents frequently found in such samples.[7] As an anionic polymer, Nafion® has been reported to be effective for eliminating anionic interferents such as ascorbic acid, uric acid and acetaminophen.[7] Blood contains endogenous ascorbic and uric acid at levels of about 0.125 and 0.33 mM, respectively whereas about 0.13 mM acetaminophen has frequently been detected. Our experimental data confirmed that the anti-interference Nafion® layer was able to circumvent acetaminophen, uric and ascorbic acids at the aforementioned levels. At such concentrations, the presence of the above-mentioned interferents provoked no signal response and the (*I*–*t*) plot obtained within 10 min was identical to the background signal. Using boron-doped diamond (BDD) electrodes rather than GC as the working electrode resulted in similar results with respect to sensitivity and detection limit.

Biosensing with other oxidases

To validate the universality of this approach, four other FAD-containing oxidases were deposited at constant current (10 μA) onto the Pt nanoparticles–CNT-modified GC electrode and their corresponding analytes were detected. Since the conversion of hydrogen peroxide is involved in all of these oxidase reactions and the applied potential was set at 700 mV (*vs.* Ag/AgCl), somewhat similar results would be expected for all the tested oxidases assuming a similar substrate conversion rate, with the exception of xanthine oxidase, which produces 2 mol of H_2O_2 for each mol of hypoxanthine. GLOx (100 U mL^{-1}) was successfully deposited (5 min) on the modified electrode and a linear relationship between current response and glutamate concentration was observed up to 100 μM (sensitivity of 29.9 ± 0.8 μA mM^{-1}, n = 9 at 95% CI, R^2 = 0.999) and a detection limit of 250 nM. The sensitivity and detection limit were similar to those reported for GOx, indicating a similar substrate conversion rate to hydrogen peroxide. Although the GLOx concentration on the electrode was about 10-fold lower than in the case of GOx, the Michaelis constant (K_M) for glutamate (2 mM) is much lower, resulting in a similar sensitivity. The linear range was not as wide as with GOx, likely due to the lower specific activity of the glutamate oxidase (25 U mg^{-1} *vs.* 185 U mg^{-1}). Good reproducibility (6%, at 95% CI) was obtained for the detection of 12 repeated glutamate analyses at 50 μM (1.55 ± 0.09 μA) and 5 μM (0.150 ± 0.008 μA). The modified electrodes were stable for at least one month, reflecting the inherent stability of the native enzyme.

AAOx (30 U mL^{-1}) deposited for 10 min onto the modified electrode exhibited a linear response to phenylalanine up to 50 μM (sensitivity of 25.4 ± 1.2 μA mM^{-1}, n = 8 at 95% CI and R^2 = 0.998) and a detection limit of 250 nM. Excellent reproducibility (1–3%, at 95% CI) was obtained for the detection of ten repeated phenylalanine analyses at 50 μM (1.13 ± 0.01 μA) and 5 μM (0.110 ± 0.003 μA). The modified electrodes were stable for a few days, which could be attributed to the inherent instability of this enzyme. LOx (100 U mL^{-1}) was deposited for 10 min onto the modified electrode for the detection of lactate. The current response was linear with lactate concentration up to 100 μM, with a sensitivity of 30.1 ± 0.3 μA mM^{-1} (n = 9 at 95% CI), R^2 = 0.999 and a detection limit of 250 nM. The detection limit was similar to that reported for a lactate sensor using LOx in a composite of poly-L-lysine.[20] Good reproducibility (7–9%, at 95% CI) was

obtained for the detection of 12 repeated lactate analyses at 50 μM (1.45 ± 0.10 μA) and 5 μM (0.138 ± 0.012 μA). Like the AAOx, the modified electrode with LOx was only stable for a few days. The sensitivity levels reported for the above four oxidases were very much alike (within 15%), indicating similar conversion rates of the starting substrates to hydrogen peroxide. Similar sensitivities were also reported for a series of oxidase enzyme electrodes based on polypyrrole films and hydrogen peroxide detection.[21]

XOx (6 U mL^{-1}) deposited for 5 min onto the modified electrode exhibited a linear response to hypoxanthine up to 5 μM (sensitivity of 0.284 ± 0.004 μA μM^{-1}, $n = 8$ at 95% CI, $R^2 = 0.999$) and a detection limit of 25 nM. Good reproducibility (5% at 95% CI) was obtained for the detection of 12 repeated hypoxanthine analyses at 200 nM (0.0512 ± 0.0024 μA). The detection limit was approximately 10-fold lower and the sensitivity was 10-fold higher than the values reported for the other analytes. These values were very similar to those reported for hydrogen peroxide. However, it was observed that xanthine (the product of the oxidation of hypoxanthine by XOx) was electroactive on the MWCNT/Pt_{nano}-modified GC electrode (in the absence of XOx), whereas hypoxanthine was not active electrochemically. The current signal (29 μA) for 100 μM xanthine was similar to that observed for 100 μM hydrogen peroxide (30.5 μM). It was likely that the detection for hypoxanthine was very sensitive since the current signal was coming from direct xanthine detection. The response curve for xanthine was the same for the modified GC electrode with or without XOx, indicating that the direct xanthine detection was much quicker than the oxidation of xanthine to uric acid and hydrogen peroxide by the enzyme. If the enzyme was anticipated to play any significant role, the current signal would have been much higher.

In brief, a biosensing platform has been constructed for the detection of analytes of various oxidase enzymes, by modifying a GC electrode with a MWCNT film followed by electrochemical deposition of Pt nanoparticles on the modified surface. The enzymes can be electrodeposited on the modified surface by a constant current technique with excellent stability and high activity. For some applications such as the monitoring of glucose in blood or urine, Nafion® can be applied to the enzyme layer to serve as a permselective membrane to circumvent the electroactive interfering species such as ascorbic acid, uric acid and acetaminophen.[7] Alternatively, such a permselective layer can be obtained by electropolymerization of a monomer such as phenol, *o*-phenylenediamine, aniline, *etc.*, and this practice has been widespread in the construction of a glucose biosensor.[1k,1m,22]

References

1 (*a*) G. Fortier, E. Brassard and D. Belanger, *Biosens. Bioelectron.*, 1990, **5**, 473–490; (*b*) Z. Zhang, H. Liu and J. Deng, *Anal. Chem.*, 1996, **68**, 1632–1638; (*c*) J. Rishpon and S. Gottesfeld, *Biosens. Bioelectron.*, 1991, **6**, 143–149; (*d*) P. N. Bartlett and J. M. Cooper, *J. Electroanal. Chem.*, 1993, **362**, 1–12; (*e*) A. Curulli and G. Palleschi, *Electroanalysis*, 1997, **9**, 1107–1112; (*f*) J. C. Vidal and J. R. Garcia, *Anal. Chim. Acta*, 1999, **383**, 213–222; (*g*) O. A. Sadik, S. Brenda, P. Joasil and J. Lord, *J. Chem. Educ.*, 1999, **76**, 967–970; (*h*) C. Malitesta, F. Palmisano, I. Torsi and P. G. Zambonin, *Anal. Chem.*, 1990, **62**, 2735–2740; (*i*) M. Quinto, I. Losito, F. Palmisano and C. G. Zambonin, *Anal. Chim. Acta*, 2000, **420**, 9–17; (*j*) C.-M. Li, C. Q. Sun, W. Chen and L. Pan, *Surf. Coat. Technol.*, 2005, **198**, 474–477; (*k*) R. Garjonyte and A. Malinauskas, *Biosens. Bioelectron.*, 2000, **15**, 445–451; (*l*) M. Situmorang, J. J. Gooding, D. B. Hibbert and D. Barnett, *Biosens. Bioelectron.*, 1998, **13**, 953–962; (*m*) S. V. Sasso, R. J. Pierce, R. Walla and A. M. Yacynych, *Anal. Chem.*, 1990, **62**, 1111–1117; (*n*) J. P. Lowry, M. Miele, R. D. O'Neill, M. G. Boutelle and M. J. Fillenz, *Neurosci. Methods*, 1998, **79**, 65–74; (*o*) D. Centonze, A. Guerrieri, C. Malitesta, F. Palmisano and P. G. Zambonin, *Fresenius' J. Anal. Chem.*, 1992, **342**, 729–733; (*p*) J. P. Lowry, K. McAteer, S. S. El Atrash, A. Duff and R. D. O'Neill, *Anal. Chem.*, 1994, **66**, 1754–1761; (*q*) F. Palmisano, A. Guerrieri, M. Quinto and P. G. Zambonin, *Anal. Chem.*, 1995, **67**, 1005–1009.

2 B. F. Y. Yon-Hin, M. Smolander, T. Crompton and C. Lowe, *Anal. Chem.*, 1993, **65**, 2067–2071; B. F. Y. Yon-Hin and C. Lowe, *J. Electroanal. Chem.*, 1994, **374**, 167–172; S. Cosnier, *Appl. Biochem. Biotechnol.*, 2000, **89**, 127–138; H. Rockel, J. Huber, R. Gleiter and W. Schuhmann, *Adv. Mater.*, 1994, **6**, 568–571; M. Hiller, C. Kranz, J. Huber, P. Bauele and W. Schuhmann, *Adv. Mater.*, 1996, **8**, 219–221.

3 W. Schulmann and R. Kittsteiner-Eberle, *Biosens. Bioelectron.*, 1991, **6**, 263–273; M. Situmorang, J. J. Gooding and D. B. Hibbert, *Anal. Chim. Acta*, 1999, **394**, 211–223; H. Dong, C. M. Li, W. Chen, Q. Zhou, Z. X. Zeng and J. H. T. Luong, *Anal. Chem.*, 2006, **78**, 7424–7432.

4 Y. Ikariyama, S. Yamauchi, T. Yukiashi and H. Ushioda, *Anal. Lett.*, 1987, **20**, 1791–1801; K. V. Johnson, *Sens. Actuators, B*, 1991, **5**, 85–89; J. Wang, I. Chen, S. B. Hocevar and B. Ogorevc, *Analyst*, 2000, **125**, 1431–1434.

5 S. S. Wang and W. R. Vieth, *Biotechnol. Bioeng.*, 1973, **15**, 93–115.

6 (*a*) E. Bakker and Y. Qin, *Anal. Chem.*, 2006, **78**, 3965–3984; (*b*) A. Merkoci, M. Pumera, X. Llopis, B. Perez, M. del Valle and S. Alegret, *TrAC, Trends Anal. Chem.*, 2005, **24**, 826–838; (*c*) J. Wang, *Analyst*, 2005, **130**, 421–426; (*d*) J. Wang, M. Musameh and Y. Lin, *J. Am. Chem. Soc.*, 2003, **125**, 2408–2409; (*e*) M. Gao, L. Dai and G. G. Wallace, *Electroanalysis*, 2003, **15**, 1089–1094; (*f*) J. Wang and M. Musameh, *Analyst*, 2003, **128**, 1382–1385; (*g*) Y. Lin, F. Lu, Y. Tu and Z. Ren, *Nano Lett.*, 2004, **2**, 191–195; (*h*) A. Callegari, S. Cosnier, M. Maracaccio, D. Paolucci, F. Paolucci, V. Georgakilas, N. Tagmatarchis, E. Vazquez and M. Prato, *J. Mater. Chem.*, 2004, **14**, 807–810; (*i*) P. P. Joshi, S. A. Merchant, Y. Wang and D. W. Schmidtk, *Anal. Chem.*, 2005, **77**, 3183–3188; (*j*) K. Besteman, J. Lee, F. Wiertz, H. Heering and C. Dekker, *Nano Lett.*, 2003, **3**, 727–730; (*k*) W. Droege, *Physiol. Rev.*, 2002, **82**, 47–95; (*l*) Z. A. Wood, L. B. Poole and P. A. Karplus, *Science*, 2003, **300**, 650–653.

7 S. Hrapovic, Y. Liu, K. B. Male and J. H. T. Luong, *Anal. Chem.*, 2004, **76**, 1083–1088.

8 S. Iijima, *Nature*, 1991, **354**, 56–58.

9 S. C. Tsang, J. J. Davis, M. L. H. Green, H. A. O. Hill, Y. C. Leung and P. J. Sadler, *J. Chem. Soc., Chem. Commun.*, 1995, 2579–2580; S. S. Tsang, Z. Guo, Y. K. Chen, M. L. H. Green, H. A. O. Hill, T. W. Hambley and P. J. Sadler, *Angew. Chem., Int. Ed. Engl.*, 1997, **36**, 2198–2220; Z. Guo, P. J. Sadler and S. C. Tsang, *Adv. Mater.*, 1998, **10**, 701–703.

10 F. Balavoine, P. Schultz, C. Richard, V. Mallouh, T. W. Ebbeson and C. Mioskowski, *Angew. Chem., Int. Ed.*, 1999, **38**, 1912–1915.

11 N. Matsumoto, X. Chen and G. S. Wilson, *Anal. Chem.*, 2002, **74**, 362–367.

12 S. A. Emr and A. M. Yacynych, *Electroanalysis*, 1995, **7**, 913–923.

13 (*a*) G. Siné, Ph.D. Thesis, 2006, 80–85, École Polytechnique Fédérale de Lausanne, Switzerland; (*b*) S. Hrapovic, Y. Liu and J. H. T. Luong, *Anal. Chem.*, 2007, **79**, 500–507.

14 Y. Liu, L. Liu and S. Dong, *Electroanalysis*, 2007, **19**, 55–59.

15 D. M. Im, D. H. Jang, H. M. Oh, C. Striebel, H. D. Wiemhoefer, G. Gaugliz and W. Goepel, *Sens. Actuators, B*, 1995, **24**, 149–155.
16 G. Lin and Y. Lin, *Electrochem. Commun.*, 2006, **8**, 252–256.
17 L. Xu, Y. Zhu, L. Tang, X. Yang and C. Li, *Electroanalysis*, 2007, **19**, 717–722.
18 D. Pan, J. Chen, S. Yao, W. Tao and L. Nie, *Anal. Sci.*, 2005, **21**, 367–371.
19 J. Li, Y.-B. Wang, J.-D. Qiu, D.-C. Sun and X.-H. Xia, *Anal. Bioanal. Chem.*, 2005, **383**, 918–922.
20 E. I. Iwouha, A. Rock and M. R. Smyth, *Electroanalysis*, 1999, **11**, 367–373.
21 W. J. Sung and Y. H. Bae, *Sens. Actuators, B*, 2006, **114**, 164–169.
22 X. Chen, N. Matsumoto, Y. Hu and G. S. Wilson, *Anal. Chem.*, 2002, **74**, 368–372.